Pergamon

Int. J. Solids Structures Vol. 33, No. 14, pp. 2023–2037, 1996

0020-7683/96 $15.00 + .00

0020-7683(95)00154-9

HOOP STRESS INTENSITY FACTOR AND CRACK-KINKING IN ANISOTROPIC BRITTLE SOLIDS

ABBAS AZHDARI and SIA NEMAT-NASSER
Center of Excellence for Advanced Materials, Department of Applied Mechanics and Engineering Sciences, University of California, San Diego, La Jolla, CA 92093, U.S.A.

(*Received* 9 *December* 1994; *in revised form* 12 *July* 1995)

Abstract—To analyze crack-kinking in an infinite, homogeneous, anisotropic, linearly elastic plane containing a central main crack, two stress intensity factors are defined. These are associated with the hoop and shear stress components at the tip of the main crack. When the hoop stress intensity factor (HSIF or $K_{\theta\theta}$) is maximum, then the shear stress intensity factor (SSIF or $K_{r\theta}$) is zero. These stress intensity factors (SIF's) are alternatives to the commonly used Modes I and II stress intensity factors (K_I and K_{II}) which uncouple for isotropic but not for anisotropic solids. Moreover, Modes I and II stress intensity factors defined at the tip of a vanishingly small kink emanating from the tip of an existing main crack ($K_I^{(k)}$ and $K_{II}^{(k)}$) are calculated by using the method that models a kink as a continuous distribution of edge dislocations. Then, the relation of HSIF (SSIF) to $K_I^{(k)}$ ($K_{II}^{(k)}$) is examined in details for various combination of relevant parameters, i.e., for different material properties, material symmetry orientations, and loadings. It is observed that for small kink angles (to the first order in the kink angle, e.g., for less than 8°) HSIF (SSIF) equals $K_I^{(k)}$ ($K_{II}^{(k)}$) to within less than 1%; this holds for much larger kink angles when the material is isotropic. As a result of this observation, for small kink angles, all field quantities at the tip of a vanishingly small kink can be obtained from the fields that exist at the tip of the initial main crack prior to kinking, i.e., to the first order in the kink angle, the Modes I and II stress intensity factors at the tip of a vanishingly small kink (just after kinking) respectively equal HSIF and SSIF (just before kinking). On the other hand, depending on loading and material anisotropy, $K_I^{(k)}$ ($K_{II}^{(k)}$) at the tip of a vanishingly small kink can deviate from HSIF (SSIF) by several hundred percent, for large kink angles. Furthermore, the K-based fracture criteria for anisotropic solids are examined in some detail. It is shown that, even for small kink angles, the study of the variation of the SIF's with the kink angle requires the corresponding complete nonlinear equation, as linearization with respect to the kink angle may produce extraneous and seemingly peculiar results.

INTRODUCTION

In the last decade, the study of failure in anisotropic materials has received considerable attention. This is due to the wider industrial application of single-crystal metals and ceramics as structural parts. Crystals of many materials, e.g., metals, quartz, and rochelle salt, are known to be anisotropic. Composite materials are also, in general, anisotropic, but often microscopically nonhomogeneous.

The redistribution of stresses in a body due to the introduction of cracks or notches may be examined by the methods of linear elastic stress analysis as a starting point. This shows that the crack-tip singularities in anisotropic and isotropic materials are of the same strength, but unlike in isotropic materials, the coupling of the stress intensity factors for anisotropic solids depends on the material properties. In addition, commonly used fracture criteria, i.e., (1) maximum K_I; (2) zero K_{II}; (3) maximum hoop stress; and (4) maximum energy-release rate, which in isotropic materials lead to similar fracture predictions (to the first order in the kink angle), do not appear to predict a similar crack propagation path in anisotropic materials. In the case of general anisotropy, the discussion of the fracture modes requires consideration of symmetries in the material properties, the applied loads, and the overall geometry of the specimen. Thus, in order to find a proper fracture criterion for anisotropic materials, coordinated theoretical and supporting experimental studies are necessary.

Within the field of fracture mechanics, especially for brittle materials, the phenomenon of crack kinking, also referred to as crack branching, is of great importance. A general anisotropic stress condition may cause crack kinking. This may be created by the anisotropy

in the material properties (e.g., single crystals and composite materials), the antisymmetry in the applied loads, or the complexity in the overall geometry. The problem of a kinked crack in isotropic materials has been investigated extensively, e.g., Chatterjee (1975), Kitagawa and Yuuki (1975), Lo (1978), Wu (1979a,b), Cotterell and Rice (1980), Nemat-Nasser (1980), Karihaloo *et al.* (1981), Hayashi and Nemat-Nasser (1981a,b), Nemat-Nasser and Horii (1982), and Sumi *et al.* (1983).

In contrast, crack kinking in anisotropic solids has received much less attention; see Miller and Stock (1989), Obata *et al.* (1989) who use the method of coupled singular integral equations, and Gao and Chiu (1992) who apply the perturbation method. Obata *et al.* (1989) studied the kinking problem in anisotropic solids numerically and confirmed the results obtained by Hayashi and Nemat-Nasser (1981a). Gao and Chiu (1992) applied the perturbation method to the problem considered by Obata *et al.* (1989) and obtained expressions for SIF's, valid to the first order in the kink angle. In the present work, for small kink angles, we capture all the field quantities at the tip of a vanishingly small kink, directly from the fields that exist prior to kinking and without using the laborious coupled singular integral equation method of Obata *et al.* (1989) or the perturbation analysis of Gao and Chiu (1992). We then examine the range of validity of the results.

We consider a central main crack embedded in an infinite, homogeneous, anisotropic and linearly elastic plane, and then define at the tip of this crack two stress intensity factors, one associated with the hoop stress, called the hoop stress intensity factor (HSIF), and the other associated with the shear stress, called the shear stress intensity factor (SSIF). The motivation for this stems from the fact that, for isotropic materials, the commonly used Mode I stress intensity factor is maximum when the corresponding Mode II stress intensity factor is zero, and this suggests that the hoop and shear stresses are appropriate candidates for defining the stress intensity factors in the anisotropic case, as suggested by Nemat-Nasser and Hori (1987) who coined the term "hoop stress intensity factor" and used this quantity to obtain the direction of the kink. Therefore, while the "hoop stress intensity factor," which is a quantity that exists prior to kinking, has been used to study crack kinking, the correspondence of HSIF and SSIF to the field quantities after kinking has not been explored in sufficient detail and in a systematic manner, to reveal all the involved interesting characteristics. This is the main objective of the present work.

The assumption that crack extension starts in the plane normal to the direction of greatest tensile stress (the maximum tensile stress criterion) was proposed by Erdogan and Sih (1963). Since the maximum tensile stress is in the direction where HSIF is maximum, the Erdogan-Sih criterion is equivalent to the maximum-HSIF criterion, although these authors do not introduce the HSIF and SSIF quantities. Otsuka *et al.* (1975) consider crack tips under mixed-mode conditions and define K_σ and K_τ as the parameters which represent the intensity of the tensile stress and the shearing stress, respectively. These parameters are defined for the isotropic case and are equivalent to HSIF and SSIF, respectively.

It will be shown that these SIF's are more descriptive in the analysis of crack kinking than the commonly used Mode I and Mode II stress intensity factors for isotropic and anisotropic solids. In the problem of crack kinking, for small kink angles, in the general anisotropic case, and for larger kink angles, in the isotropic case, HSIF and SSIF approximate the values of Mode I and Mode II stress intensity factors at the tip of a vanishingly small kink ($K_I^{(k)}$ and $K_{II}^{(k)}$) within a reasonable accuracy. We demonstrate that the stress intensity factors calculated at the tip of a vanishingly small kink (assuming small kink angles) by Obata *et al.* (1989) and Gao and Chiu (1992) are simply the HSIF and SSIF defined at the tip of the main crack. In other words, we show that, once the crack problem without a kink is solved, then the stress intensity factors and the energy release rate can readily be evaluated for an infinitesimally small kink, with the aid of the expressions for the hoop and shear stress intensity factors defined at the tip of the main crack, without a need for laborious asymptotic analysis. Using these hoop and shear stress intensity factors, the corresponding results of Obata *et al.* (1989) (for small kink angles) and Gao and Chiu (1992) (for all cases that they considered) can be easily reproduced.

In the course of this work, it was observed that the *linearized* version of the equation obtained for the kink angle by the maximization of K_I (or by setting $K_{II} = 0$) at the tip of

an infinitesimally small kink may produce physically unreasonable predictions for the kink direction (Gao and Chiu, 1992). This is, however, extraneous to the actual solution of the original nonlinear equation, as will be shown in the present work. Indeed, the linearized equation yields an unbounded optimal kink angle when $C_{yy}/C_{xx} = 4$, whereas no such singular behavior is predicted when the full nonlinear equation is used to calculate this optimal kink angle. Even the second- or third-order approximations of this expression may lead to some other false conclusions. We will show that, from an analytical point of view, the K-based fracture criteria are as viable as any other criterion, and that the physical relevance of these and other fracture criteria needs to be settled experimentally. In addition, we examine illustrations which show large deviations (e.g., several hundred percent) between the HSIF and SSIF and the actual SIF's at the tip of a vanishingly small kink. In a work in progress, we have observed that the energy-release rate can be calculated either in terms of the hoop and shear stresses which exist prior to kinking or in terms of the stress fields ahead of an existing vanishingly small kink, both techniques yielding exactly the same value for the energy-release rate at the tip of a vanishingly small kink of *any* kink angle.

FORMULATION

Statement of problem

Consider an infinite, anisotropic, homogeneous, linearly elastic plane which contains a traction-free central crack of length $2a$. The fixed rectangular Cartesian coordinate system, x_1-x_2, is used where the x_1-axis coincides with the crack, as shown in Fig. 1. A supplementary Cartesian coordinate system, x-y, is also used to indicate the material coordinate system. In what follows, a prime denotes differentiation with respect to the corresponding argument, and an overbar represents the complex conjugate of the corresponding variable. Let the body be in the state of plane-stress or plane-strain under uniform farfield tractions σ^∞ acting at an angle β relative to the crack. This applied tension, σ^∞, is equivalent to two tensile stresses and a shear stress, applied at infinity, as follows:

$$\sigma^\infty_{11} = \sigma^\infty \cos^2\beta, \quad \sigma^\infty_{22} = \sigma^\infty \sin^2\beta, \quad \sigma^\infty_{12} = \sigma^\infty \sin\beta\cos\beta. \tag{1a–c}$$

Therefore, the farfield loading is non-symmetric unless $\beta = \pm 90^\circ$ (or $\beta = 0^\circ$, which is uninteresting).

Some basics of anisotropic elasticity and its application to the present problem

For plane-stress deformations of an anisotropic, homogeneous, linearly elastic solid, the strain-stress relations in the x_1, x_2-plane are:

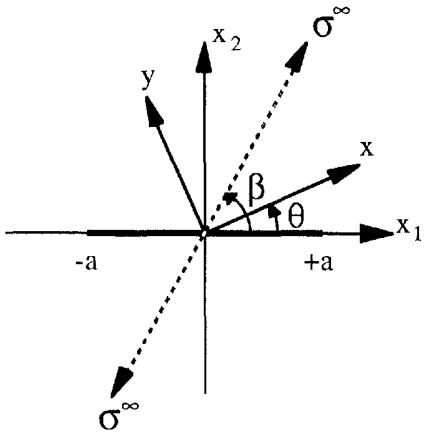

Fig. 1. Geometry, coordinate systems, and loading direction.

$$\varepsilon_{11} = C_{11}\sigma_{11} + C_{12}\sigma_{22} + C_{16}\sigma_{12},$$
$$\varepsilon_{22} = C_{12}\sigma_{11} + C_{22}\sigma_{22} + C_{26}\sigma_{12},$$
$$2\varepsilon_{12} = C_{16}\sigma_{11} + C_{26}\sigma_{22} + C_{66}\sigma_{12}, \tag{2a–c}$$

where $C_{ij} = C_{ji}$; $i, j = 1, 2, 6$ are the relevant elements of the compliance matrix of the material. From a mathematical point of view, the plane-strain problems are obtained by simply changing the compliance matrix from C_{ij} to $C_{ij} - (C_{i3}C_{j3})/C_{33}$ in (2a–c). It has been shown that (Lekhnitskii, 1963; Savin, 1961) the problems of two-dimensional anisotropic elasticity can be conveniently formulated in terms of two independent analytic functions, $\phi_1(z_1)$ and $\phi_2(z_2)$. The complex variables z_1 and z_2 are

$$z_i = x_1 + \mu_i x_2, \quad i = 1, 2; \tag{3}$$

where μ_1 and μ_2 are the roots of the characteristic equation,

$$C_{11}\mu^4 - 2C_{16}\mu^3 + (2C_{12} + C_{66})\mu^2 - 2C_{26}\mu + C_{22} = 0. \tag{4}$$

Due to the positive-definiteness of the elastic energy, the characteristic equation has either complex or purely imaginary roots which are pairwise complex conjugates, i.e., $\mu_3 = \overline{\mu_1}$ and $\mu_4 = \overline{\mu_2}$. We choose μ_1 and μ_2 such that their imaginary parts are positive. Note that the isotropic case may be regarded as the limiting case for which $\mu_1 = \mu_2 = i = \sqrt{-1}$.

The stresses and displacements are as follows

$$\sigma_{11} = 2\,\mathrm{Re}\,[\mu_1^2\phi_1'(z_1) + \mu_2^2\phi_2'(z_2)],$$
$$\sigma_{22} = 2\,\mathrm{Re}\,[\phi_1'(z_1) + \phi_2'(z_2)],$$
$$\sigma_{12} = -2\,\mathrm{Re}\,[\mu_1\phi_1'(z_1) + \mu_2\phi_2'(z_2)], \tag{5a–c}$$

$$u_1 = 2\,\mathrm{Re}\,[p_1\phi_1(z_1) + p_2\phi_2(z_2)] \quad \text{and} \quad u_2 = 2\,\mathrm{Re}\,[q_1\phi_1(z_1) + q_2\phi_2(z_2)], \tag{6a,b}$$

where p_i and q_i are

$$p_i = C_{11}\mu_i^2 + C_{12} - C_{16}\mu_i \quad \text{and} \quad q_i = C_{12}\mu_i + \frac{C_{22}}{\mu_i} - C_{26}. \tag{7a,b}$$

Therefore, once the stress functions, $\phi_1(z_1)$ and $\phi_2(z_2)$, for a particular boundary-value problem are found, then the stresses and displacements are readily calculated using (5–7). For example, for the present problem (an infinitely extended plane containing a central crack, loaded uniformly at infinity), the stress functions are given by (Savin, 1961),

$$\phi_i(z_i) = Q_i(z_i - \sqrt{z_i^2 - a^2}), \quad i = 1, 2, \tag{8}$$

where Q_1 and Q_2 (when the loading is such that the crack is *open*) are

$$Q_1 = \frac{\sigma^\infty(2\mu_2 \sin^2\beta + \sin 2\beta)}{4(\mu_1 - \mu_2)}, \quad Q_2 = -\frac{\sigma^\infty(2\mu_1 \sin^2\beta + \sin 2\beta)}{4(\mu_1 - \mu_2)}. \tag{9a,b}$$

Considering now (5), the stresses become

$$\sigma_{11} = \sigma^\infty \cos^2\beta + 2\,\mathrm{Re}\,[\mu_1^2\phi_1'(z_1) + \mu_2^2\phi_2'(z_2)],$$
$$\sigma_{22} = \sigma^\infty \sin^2\beta + 2\,\mathrm{Re}\,[\phi_1'(z_1) + \phi_2'(z_2)],$$

$$\sigma_{12} = \sigma^{\infty} \sin\beta\cos\beta - 2\,\mathrm{Re}\,[\mu_1\phi_1'(z_1) + \mu_2\phi_2'(z_2)], \tag{10a–c}$$

where from (8),

$$\phi_i'(z_i) = Q_i\left(1 - \frac{z_i}{\sqrt{z_i^2 - a^2}}\right), \quad i = 1,2 \tag{11}$$

are the derivatives of the stress functions. Note that the terms which involve σ^{∞} in (10) account for the uniform stresses applied at infinity, i.e., as $|z_i|$ goes to infinity.

Using (6), one can obtain the displacements at any point on the plane. Crack opening displacements, COD's, are defined as the jump in the displacements along the crack line (on the crack line $x_2 = 0$ and thus, $z_1 = z_2 = x_1$). The final expressions for crack opening displacements, $[u_1]$ and $[u_2]$, are:

$$[u_1] = 2C_{11}[(\alpha_1\beta_2 + \alpha_2\beta_1)\sigma_{22}^{\infty} + (\beta_1 + \beta_2)\sigma_{12}^{\infty}]\sqrt{a^2 - x_1^2}, \tag{12}$$

$$[u_2] = 2C_{11}[\{(\alpha_1^2 + \beta_1^2)\beta_2 + (\alpha_2^2 + \beta_2^2)\beta_1\}\sigma_{22}^{\infty} + (\alpha_1\beta_2 + \alpha_2\beta_1)\sigma_{12}^{\infty}]\sqrt{a^2 - x_1^2}, \tag{13}$$

where $\mu_1 = \alpha_1 + i\,\beta_1$ and $\mu_2 = \alpha_2 + i\,\beta_2$.

The x_2-component of COD (13) is physically reasonable only when $[u_2] > 0$. This ensures no overlap of the material. Analytically, this condition can be written as; see (13),

$$\{(\alpha_1^2 + \beta_1^2)\beta_2 + (\alpha_2^2 + \beta_2^2)\beta_1\}\sigma_{22}^{\infty} + (\alpha_1\beta_2 + \alpha_2\beta_1)\sigma_{12}^{\infty} \geqslant 0. \tag{14}$$

It is noteworthy that, according to (9–11), when the plane is loaded in the x_1-direction, i.e., when $\beta = 0$, then $\phi_1' = \phi_2' = 0$ and therefore one can deduce that a crack in the direction of the tensile stress in an anisotropic medium does not influence the stress state. In view of this, the stress component collinear with the crack, σ_{11}^{∞}, does not appear in the final equations which characterize the stress intensity factors at the tip of the main crack.

Hoop and shear stress intensity factors (HSIF and SSIF)

Consider now a polar coordinate system at the crack tip, Fig. 2, such that $x_1 = a + r\cos\omega$ and $x_2 = r\sin\omega$, which together with (3) result in a new form for the z_i's,

$$z_i = a + r(\cos\omega + \mu_i\sin\omega), \quad i = 1,2. \tag{15}$$

Using (15) in (11), the derivative of the stress function near the crack tip is obtained as

$$\phi_i'(z_i) = Q_i\left(1 - \frac{1}{\sqrt{2\pi r}}\frac{\sqrt{\pi a}}{\sqrt{(\cos\omega + \mu_i\sin\omega)}} + f(O(r^{1/2}), \omega)\right), \quad i = 1,2. \tag{16}$$

As is well known, this shows that the stresses at the crack tip are square-root singular.

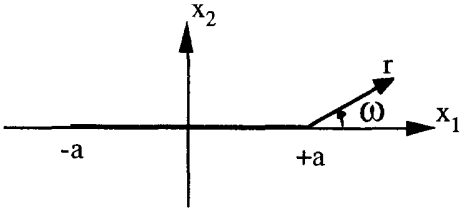

Fig. 2. Polar coordinates at the crack tip.

The hoop and the shear stresses at an angle ω near the right tip of the crack, Fig. 2, are obtained from the following relations between Cartesian and polar coordinates (the Mohr circle):

$$\sigma_{\omega\omega} = (\sigma_{22}-\sigma_{11})\cos^2\omega+\sigma_{11}-2\sigma_{12}\cos\omega\sin\omega,$$
$$\sigma_{r\omega} = (\sigma_{22}-\sigma_{11})\sin\omega\cos\omega+\sigma_{12}(\cos^2\omega-\sin^2\omega). \tag{17a,b}$$

Substitution of (10) into (17) now gives the following compact relations for the hoop and shear stresses:

$$\sigma_{\omega\omega} = 2\,\mathrm{Re}\,[\phi_1'(z_1)(c+\mu_1 s)^2+\phi_2'(z_2)(c+\mu_2 s)^2]+\sigma^\infty\sin^2 v,$$
$$\sigma_{r\omega} = 2\,\mathrm{Re}\,[\phi_1'(z_1)(c+\mu_1 s)(s-\mu_1 c)+\phi_2'(z_2)(c+\mu_2 s)(s-\mu_2 c)]+\sigma^\infty\sin v\cos v, \tag{18a,b}$$

where $c\equiv\cos\omega$, $s\equiv\sin\omega$, and $v=\beta-\omega$.

Define the following two stress intensity factors associated with the hoop and shear stresses at an arbitrary angle ω:

$$K_{\omega\omega}\equiv\lim_{r\to 0}(\sqrt{2\pi r}\sigma_{\omega\omega}),\quad K_{r\omega}\equiv\lim_{r\to 0}(\sqrt{2\pi r}\sigma_{r\omega}). \tag{19a,b}$$

Computation of these two quantities requires the following limiting values of the stress functions:

$$\lim_{r\to 0}(\sqrt{2\pi r}\phi_i'(z_i)) = \frac{-Q_i\sqrt{\pi a}}{\sqrt{\cos\omega+\mu_i\sin\omega}}. \tag{20}$$

Substituting (18) into (19) and using (20), the stress intensity factors become

$$K_{\omega\omega} = -\sqrt{\pi a}\,\mathrm{Re}\left[\frac{1}{\mu_1-\mu_2}\{\sigma_{22}^\infty[\mu_2(c+\mu_1 s)^{3/2}-\mu_1(c+\mu_2 s)^{3/2}]\right.$$
$$\left.+\sigma_{12}^\infty[(c+\mu_1 s)^{3/2}-(c+\mu_2 s)^{3/2}]\}\right], \tag{21a}$$

$$K_{r\omega} = -\sqrt{\pi a}\,\mathrm{Re}\left[\frac{1}{\mu_1-\mu_2}\{\sigma_{22}^\infty[\mu_2(c+\mu_1 s)^{1/2}(s-\mu_1 c)-\mu_1(c+\mu_2 s)^{1/2}(s-\mu_2 c)]\right.$$
$$\left.+\sigma_{12}^\infty[(c+\mu_1 s)^{1/2}(s-\mu_1 c)-(c+\mu_2 s)^{1/2}(s-\mu_2 c)]\}\right]. \tag{21b}$$

Note that by setting ω equal to zero, the common expressions for the stress intensity factors are obtained,

$$K_I^\infty = K_{\omega\omega}(\omega=0) = \sigma_{22}^\infty\sqrt{\pi a},\quad K_{II}^\infty = K_{r\omega}(\omega=0) = \sigma_{12}^\infty\sqrt{\pi a}. \tag{22a,b}$$

Thus, for anisotropic materials, HSIF and SSIF are more convenient quantities than the commonly used Modes I and II stress intensity factors, since HSIF and SSIF uncouple the Modes I and II on planes at suitable angles relative to the main crack; see Fig. 2.

The HSIF and SSIF can be written as a linear combination of the apparent stress intensity factors, K_I^∞ and K_{II}^∞, as

$$K_{\omega\omega} = K_{11}K_I^\infty + K_{12}K_{II}^\infty, \quad K_{r\omega} = K_{21}K_I^\infty + K_{22}K_{II}^\infty, \tag{23a,b}$$

where

$$K_{11} = \mathrm{Re}\left[\frac{1}{\mu_2-\mu_1}\{\mu_2(c+\mu_1 s)^{3/2} - \mu_1(c+\mu_2 s)^{3/2}\}\right],$$

$$K_{12} = \mathrm{Re}\left[\frac{1}{\mu_2-\mu_1}\{(c+\mu_1 s)^{3/2} - (c+\mu_2 s)^{3/2}\}\right],$$

$$K_{21} = \mathrm{Re}\left[\frac{1}{\mu_2-\mu_1}\{\mu_2(c+\mu_1 s)^{1/2}(s-\mu_1 c) - \mu_1(c+\mu_2 s)^{1/2}(s-\mu_2 c)\}\right],$$

$$K_{22} = \mathrm{Re}\left[\frac{1}{\mu_2-\mu_1}\{(c+\mu_1 s)^{1/2}(s-\mu_1 c) - (c+\mu_2 s)^{1/2}(s-\mu_2 c)\}\right]. \tag{24a–d}$$

Equations (21a,b) show that the hoop and shear stress intensity factors are functions of geometry, loading, material properties, and the direction ω. As was mentioned earlier, the far-field stress collinear with the crack, i.e., loading in the x_1-direction, does not appear in (21). It should be noted that (21) can also be deduced from eqn (77) of Gao and Chiu (1992) who used a laborious perturbation method to derive it. To this end, note from (18) and (19) that the hoop and shear stresses in the vicinity of the crack tip take on the form

$$\sigma_{\omega\omega} = \frac{K_{\omega\omega}}{\sqrt{2\pi r}}, \quad \sigma_{r\omega} = \frac{K_{r\omega}}{\sqrt{2\pi r}}. \tag{25a,b}$$

The angle at which the hoop stress is maximum, "ω_c", can be computed by maximizing HSIF, (21a), with respect to ω. This leads to

$$\mathrm{Re}\left[\frac{1}{\mu_1-\mu_2}\{[\mu_2(c+\mu_1 s)^{1/2}(s-\mu_1 c) - \mu_1(c+\mu_2 s)^{1/2}(s-\mu_2 c)] + \alpha[(c+\mu_1 s)^{1/2}(s-\mu_1 c) - (c+\mu_2 s)^{1/2}(s-\mu_2 c)]\}\right] = 0, \tag{26}$$

where α, defined as

$$\alpha = \sigma_{12}^\infty/\sigma_{22}^\infty = K_{II}^\infty/K_I^\infty, \tag{27}$$

may be considered as a measure of *mode mixity*. Note that (26) also results if SSIF given by (21b), is simply set equal to zero. This is because the derivative of HSIF with respect to "ω" is proportional to SSIF, i.e., $2\,\partial K_{\omega\omega}/\partial\omega = -3\,K_{r\omega}$. Hence, *when* HSIF is *extremum*, SSIF is *exactly zero*. Therefore, the maximum-$K_{\omega\omega}$ and the zero-$K_{r\omega}$ fracture criteria yield identical results in this case. The unknown in (26), ω_c, the angle at which the hoop stress is maximum, can be found numerically. This angle is a function of the material properties and the ratio of the two far-field stresses (α). This angle may be considered as the angle at which the crack would propagate under the applied loads, provided that the material resistance to cracking is independent of the orientation ω. (This assumption must be verified by experimental results and is *not* expected to hold for anisotropic materials.) If the remote applied stress is in the x_2-direction, i.e., if $\sigma_{12}^\infty = 0$, then (26) simplifies to

$$\mathrm{Re}\left[\frac{1}{\mu_1-\mu_2}\{\mu_2(c+\mu_1 s)^{1/2}(s-\mu_1 c)-\mu_1(c+\mu_2 s)^{1/2}(s-\mu_2 c)\}\right]=0. \tag{28}$$

Under this condition, the angle of the maximum HSIF depends only on the material properties. Note that the angle "ω_c", the root of (26) and/or (28), is obtained such that HSIF is maximum in that direction and hence, the SSIF vanishes there. In this manner, the two SIF's are *decoupled* along the ω_c-direction.

SELECTION OF MATERIAL PROPERTIES

Numerical calculations are performed for the special case of orthotropic materials, where $C_{16}=C_{26}=0$; this then allows direct comparison with the results of Obata *et al.* (1989) and Gao and Chiu (1992). Then, the characteristic eqn (4) reduces to

$$C_{xx}\hat{\mu}^4+(2C_{xy}+C_{ss})\hat{\mu}^2+C_{yy}=0, \tag{29}$$

where C_{xx}, C_{yy}, C_{xy}, C_{ss}, and $\hat{\mu}$ are the equivalent symbols for C_{11}, C_{22}, C_{12}, C_{66}, and μ, respectively; see the x, y- and the x_1, x_2-coordinate systems in Fig. 1. The on-axis orthotropic constants can be written in terms of Young's moduli, the shear modulus, and Poisson's ratio as:

$$C_{xx}=\frac{1}{E_{xx}},\quad C_{yy}=\frac{1}{E_{yy}},\quad C_{ss}=\frac{1}{E_{ss}},\quad C_{xy}=-\frac{\nu_x}{E_{xx}}=-\frac{\nu_y}{E_{yy}}. \tag{30}$$

The solution of (29) is:

$$\hat{\mu}_{1,2}=\frac{i}{\sqrt{2}}[(q+p)^{1/2}\pm(q-p)^{1/2}],\quad \text{for } q\geqslant p, \tag{31a}$$

$$\hat{\mu}_{1,2}=\frac{i}{\sqrt{2}}[(p+q)^{1/2}\pm i(p-q)^{1/2}],\quad \text{for } q\leqslant p, \tag{31b}$$

where $p^2=C_{yy}/C_{xx}=E_{xx}/E_{yy}$ and $q=(2C_{xy}+C_{ss})/2C_{xx}=E_{xx}/2E_{ss}-\nu_x$. Once the $\hat{\mu}$'s are calculated by (31), one can use the transformation formula

$$\mu_i=\frac{\hat{\mu}_i\cos(-\theta)-\sin(-\theta)}{\cos(-\theta)+\hat{\mu}_i\sin(-\theta)} \tag{32}$$

to transform $\hat{\mu}$ (in the x, y-coordinate system) to μ (in the x_1, x_2-coordinate system). In order to be consistent with the numerical results of Obata *et al.* (1989) and Gao and Chiu (1992), we further restrict the orthotropy of the material to $C_{ss}=2(C_{xx}-C_{xy})$, unless explicitly stated otherwise. This leads to $p=\sqrt{C_{yy}/C_{xx}}=\sqrt{E_{xx}/E_{yy}}$ and $q=1$. It is worthy to note that the two parameters p and q take on the value of unity for isotropic materials, and therefore they may be considered as a measure of the anisotropy of the material.

RESULTS AND DISCUSSION

In what follows, the main crack is assumed to be in the x_1-direction. The asymmetry is caused by either the material orientation or loading or both. The hoop stress intensity factors are calculated by (21a,b). Expression "$\omega_c(K_m)$" denotes the angle at which the HSIF is maximum (or SSIF is zero). Moreover, the ratio of compliances in the x-direction and y-direction is denoted by $r^{xy}=C_{xx}/C_{yy}$ (or $r^{yx}=C_{yy}/C_{xx}$). Furthermore, HSIF and SSIF are non-dimensionalized so that HSIF takes on the value of "one" at

$\omega = 0$. Setting $\omega = 0$ in (21a), gives the required terms for non-dimensionalization, as $K_0 \equiv K_{\omega\omega}(\omega = 0) = K_I^{\infty} = \sigma_{22}^{\infty}\sqrt{\pi a}$.

Comparison of HSIF and SSIF with $K_I^{(k)}$ *and* $K_{II}^{(k)}$

(a) *Calculation of* $K_I^{(k)}$ *and* $K_{II}^{(k)}$. Modes I and II stress intensity factors at the tip of a vanishingly small kink emanating from the tip of the main crack, $K_I^{(k)}$ and $K_{II}^{(k)}$, are calculated using the method that models the kink as a continuous distribution of edge dislocations; Lo (1978). Obata *et al.* (1989) applied this method to solve the kink problem in an anisotropic solid. We use the formulation by Obata *et al.* (1989) to calculate $K_I^{(k)}$ and $K_{II}^{(k)}$. In brief, the method results in a system of coupled singular integral equations where the non-singular parts of the dislocation density functions (B_x and B_y) are the unknowns of the problem. In order to solve this system numerically, B_x and B_y are interpolated using "N" piece-wise quadratic polynomials; see Gerasoulis (1982). This leads to a system of $2(2N+1)$ algebraic linear equations. Once this system is solved, the values of B_x and B_y at $2N+1$ district points along the kink line are known. Obata *et al.* (1989) show that:

$$K_I^{(k)} = \pi\sqrt{\frac{2\pi}{L}}[M_{11}B_x(L) + M_{12}B_y(L)],$$

$$K_{II}^{(k)} = \pi\sqrt{\frac{2\pi}{L}}[M_{21}B_x(L) + M_{22}B_y(L)], \tag{33a,b}$$

where L is the kink length and M_{ij}'s are some known functions of the material properties and the kink angle ω; see Fig. 3.

For a vanishingly small kink, the ratio of the kink to the main crack length is chosen to be, $L/a < 10^{-6}$. An alternative way for handling the vanishingly small kink is to consider $L/a \ll 1$, and then show that B_x and B_y along the kink length are proportional to $\sqrt{L}$; see Azhdari (1995). Thus, $K_I^{(k)}$ and $K_{II}^{(k)}$ become independent of length L. As a result, the numerical routine is independent of the kink length, which increases the accuracy and the efficiency of the calculation. Hence, the numerical values of $K_I^{(k)}$ and $K_{II}^{(k)}$ are calculated, using both methods. For $N > 100$, convergence for the values of $K_I^{(k)}$ and $K_{II}^{(k)}$ is observed.

(b) *General anisotropic case.* Here, comparison between HSIF (SSIF) and $K_I^{(k)}$ ($K_{II}^{(k)}$) is made using two sources; (1) the first-order approximation in the kink angle reported by Gao and Chiu (1992); and (2) the numerical results of Obata *et al.* (1989). Gao and Chiu (1992) applied the perturbation method on the solution of a straight crack in an infinite plane. A kink at a small angle can be simulated by this method. The result is eqn (77) of Gao and Chiu (1992), which gives $K_I^{(k)}$ and $K_{II}^{(k)}$ to the first order in the kink angle, ω. As was mentioned earlier, (21) of the present work is identical to (77) of Gao and Chiu (some algebraic manipulations are required). Therefore, *for small kink angles*, the HSIF and SSIF are identical to the Modes I and II stress intensity factors defined at the tip of a vanishingly small kink, $K_I^{(k)}$ and $K_{II}^{(k)}$. This is true for any material property and loading condition.

It is concluded by Gao and Chiu (1992) that, in the limiting case of a crack with an infinitesimal branch length, comparison with numerical results reported in the literature

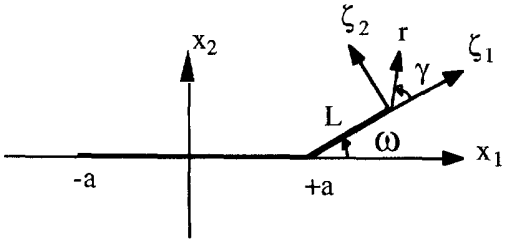

Fig. 3. Coordinate system for a kinked crack.

indicates that the perturbation solutions are accurate over the full range of practically important branch angles, up to 150°. While a cursory comparison between the results of eqn (77) of Gao and Chiu (1992) with a few examples reported by Obata *et al.* (1989) may seem to support this conclusion, it will be shown below that, for large kink angles, the first-order solutions (either (77) of Gao and Chiu (1992) or our (21a,b)) do not, in general, yield the values of $K_I^{(k)}$ and $K_{II}^{(k)}$ with any reasonable accuracy.

In order to demonstrate how different HSIF (SSIF) and $K_I^{(k)}$ ($K_{II}^{(k)}$) can indeed be, consider the following example where the involved parameters are taken as: $E_{yy}/E_{xx} = 0.125$, $E_{ss}/E_{xx} = 0.10$, $\sigma_{22}^{\infty}/E_{xx} = 4\times10^{-3}$, $\sigma_{12}^{\infty}/E_{xx} = 6\times10^{-3}$, $v_y = 0.25$, $\theta = 60°$, $\omega = -150°$, and $N = 100$. With these parameters, one obtains: HSIF $= 10.69\times10^{-3}$ and $K_I^{(k)} = 27.80\times10^{-3}$, SSIF $= -28.39\times10^{-3}$ and $K_{II}^{(k)} = -17.68\times10^{-3}$. As is seen, in this example, the actual K_I (i.e., $K_I^{(k)}$) is more than 2.5 times that calculated using the first-order asymptotic solution of the hoop stress intensity factor (HSIF). A similar discrepancy exists between $K_{II}^{(k)}$ and SSIF. Of course, under certain conditions (material property or material symmetry orientation or loading conditions), (21a,b) may yield accurate values for $K_I^{(k)}$ and $K_{II}^{(k)}$ even if the kink angle is large. But, in general, this conclusion is not valid.

We will examine the range of the kink angle for which the first-order asymptotic solution or the HSIF and SSIF yield accurate estimates of $K_I^{(k)}$ and $K_{II}^{(k)}$. This depends not only upon the value of the kink angle, but also on other parameters, e.g., the material properties (for example, E_{xx}, E_{yy}), material symmetry orientation θ, and the applied stress σ^{∞}. To examine this dependency, a wide range of such parameters is selected and certain possible combinations of these parameters are considered. In the numerical calculations, the following values are used: main crack length $2a = 2.0$; kink length $L = 0.000001$; Poisson's ratio $v_y = 0.25$; shear modulus $E_{ss} = 0.4$; the number of piece-wise quadratic polynomials used for the numerical calculations $N = 100$; Young's modulus in the x-direction $E_{xx} = 1, 2, 5, 10$; Young's modulus in the y-direction $E_{yy} = 1, 2, 5, 10$; tensile load at infinity $\sigma_{22}^{\infty} = 0, 1, 2, 0.01$; shear load at infinity $\sigma_{12}^{\infty} = 0, 1, 2, 0.01$; and material symmetry orientation $\theta = -30°, 0°, +30°$. Finally, the kink angle is varied from $-120°$ to $+120°$ with increments of 5°. Note that the elastic constants and the stresses applied at infinity are non-dimensionalized with respect to E_{xx}, with the stress components being magnified by a suitable factor, since the solution is proportional to the magnitude of the stress.

The difference between HSIF (SSIF) and $K_I^{(k)}$ ($K_{II}^{(k)}$) is represented by: $(\text{Diff})_{\omega\omega} = 100[(K_I^{(k)} - K_{\omega\omega})/K_I^{(k)}]$ and $(\text{Diff})_{r\omega} = 100[(K_{II}^{(k)} - K_{r\omega})/K_{II}^{(k)}]$. Certain possible combinations of the various parameters have been considered and for each combination the range of the kink angle within which these relative differences are less than 1%, has been calculated; the tabulated results are given in Azhdari (1995). These results show that, in general, when the kink angle is between $-8°$ and $+8°$, then the difference between HSIF (SSIF) and $K_I^{(k)}$ ($K_{II}^{(k)}$) is less than 1.0%. This range ($-8°$ to $+8°$) widens as E_{xx} approaches E_{yy}, and narrows for very large or very small ratios of E_{xx}/E_{yy}. In general, the larger the kink angle, the larger becomes the difference between HSIF (SSIF) and $K_I^{(k)}$ ($K_{II}^{(k)}$). There are many cases for which this difference is very small (around 1%) even for kink angles as large as 100°. This happens to be the case for the examples worked out by Obata *et al.* (1989), which have been used by Gao and Chiu (1992), to infer that the difference between these quantities is small even for kink angles as large as 150°.

(c) *Isotropic case.* Let us now compare HSIF (SSIF) with $K_I^{(k)}$ ($K_{II}^{(k)}$) for the isotropic case. For this, calculate the limiting values of the expressions given in (24) when $\mu_1 = \mu_2 = i = \sqrt{-1}$:

$$K_{11} = \frac{1}{4}\left[3\cos\frac{\omega}{2} + \cos\frac{3\omega}{2}\right], \quad K_{12} = -\frac{3}{4}\left[\sin\frac{\omega}{2} + \sin\frac{3\omega}{2}\right],$$

$$K_{21} = \frac{1}{4}\left[\sin\frac{\omega}{2} + \sin\frac{3\omega}{2}\right], \quad K_{22} = \frac{1}{4}\left[\cos\frac{\omega}{2} + 3\cos\frac{3\omega}{2}\right]. \tag{34a,b}$$

These expressions are identical to those in the Irwin-Williams solution; see Williams (1957). For the isotropic case, the asymmetry is only due to the asymmetric loading; see Fig. 1 and eqn (1). This renders HSIF (SSIF) close to $K_I^{(k)}$ ($K_{II}^{(k)}$) even at relatively large kink angles. For example, when the loading is a pure shear (the most asymmetric case), the investigation shows that, for kink angles up to $\pm 38^\circ$ ($\pm 18^\circ$), the relative difference between HSIF and $K_I^{(k)}$ (SSIF and $K_{II}^{(k)}$) is less than 1%. Obviously, for the cases when the loading is less asymmetric (some tensile load is applied), the range of the kink angles within which HSIF (SSIF) is in good agreement with $K_I^{(k)}$ ($K_{II}^{(k)}$) is larger.

According to the maximum-K_I fracture criterion (or equivalently zero-K_{II}), a crack in an isotropic solid would kink at an angle not greater than $\pm 77^\circ$; these angles are calculated from (33). Therefore, for all practical purposes in the fracturing of isotropic brittle solids, the kink angles to be considered are between $+77^\circ$ and -77°. Now, if HSIF and SSIF of (23) and (34), are used, then the limiting kink angles of $\pm 77^\circ$ change to $\pm 71^\circ$ which is in error by less than 10%. It is interesting to note that, for pure shear, the relative difference between SSIF and $K_{II}^{(k)}$ is more than 100%, but SSIF is zero at an angle close to that which makes $K_{II}^{(k)}$ zero. Hence, for isotropic solids, the maximum-HSIF and/or the zero-SSIF fracture criteria predict kink angles close to those predicted by the maximum-$K_I^{(k)}$ and/or the zero-$K_{II}^{(k)}$ criteria.

K-based fracture criteria

We have shown that eqn (77) of Gao and Chiu (1992) and/or our eqn (21) yield accurate estimates of $K_I^{(k)}$ and $K_{II}^{(k)}$ *only for small values of the kink angle*. In order to investigate the K-based fracture criterion, we consider (26) derived from (21). This equation yields the kink orientation which renders K_I maximum and K_{II} zero. We examine the variation in the optimal kink angle predicted by various approximate versions of the nonlinear eqn (26). To the third-order approximation in ω (for illustration, assume that $C_{ss} = 2(C_{xx} - C_{xy})$, and that θ is zero or very small, i.e., the material- and body-coordinates almost coincide), (26) becomes:

$$(20 - 10p - 3p^2)\omega^3 + 6\alpha(8-p)\omega^2 - 24(2-p)\omega - 48\alpha = 0, \tag{35}$$

where α and p are defined in (27) and (31), respectively. By neglecting ω^3 and ω^2, (35) reduces to

$$\omega = \frac{-2\alpha}{(2-p)} = \frac{-2K_{II}^{\infty}/K_I^{\infty}}{(2-\sqrt{C_{yy}/C_{xx}})}, \tag{36}$$

which is the same as eqn (84) of Gao and Chiu (1992). This equation suggests peculiar results which are extraneous to the solution of the original nonlinear eqn (26). According to (36), ω becomes unbounded at $p = 2$. In other words, when the ratio of compliances in the y- and x-directions is 4, the branch angle ω predicted by the K-based fracture criterion is *infinite*. As is seen, this prediction is a result of the linearization rather than the corresponding fracture criterion. For example, the second- or third-order equations obtained from (35) are not ill-conditioned at $p = 2$, but may have singularities at other values of p, depending on the value of α. Indeed, when (26) is solved numerically (without approximation) for ω, *no singularity results for any loading and any material orientation*. For the isotropic case, $p = 1$, (35) provides an estimate which is accurate to the third order in the branch angle ω. For this case, we have

$$7\omega^3 + 42\alpha\omega^2 - 24\omega - 48\alpha = 0 \tag{37}$$

which yields accurate values for ω even when α is not small (when the applied shear is relatively large). Note that, by ignoring ω^3 and ω^2 in (37), one arrives at $\omega = -2\alpha$, a well-established formula for the branch angle in isotropic elastic solids for sufficiently small α; e.g., Hayashi and Nemat-Nasser (1981b). For example, for $\alpha = 0.25$, (37) yields the value

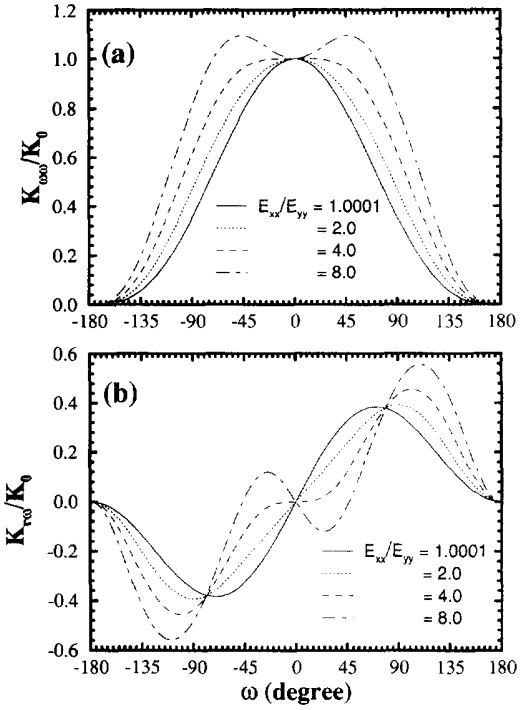

Fig. 4. Variation of: (a) HSIF and (b) SSIF vs ω for $\theta = 0^\circ$ and $\alpha = 0.0$ (pure tensile stress).

of ω with less than 1% error, while the linearized estimate of $\omega = -2\alpha$ involves an error of about 12%. It is worthy to note that an alternative way to obtain the formula $\omega = -2\alpha$ is to maximize the HSIF (23a) with respect to ω and then linearize the result for small ω's. In this process, (27) and (34a) are used.

Next, let us investigate the variation of the extremum values of HSIF denoted K_I by Gao and Chiu (1992), as the ratio r^{yx} exceeds 4. As r^{yx} is increased, at a certain critical value, say, at $r^{yx} = r_c^{yx}$, depending on the values of θ and α, the curvature of the HSIF-curve with respect to ω changes, as is illustrated in Fig. 4a. When r^{yx} is less than r_c^{yx}, the curve has one maximum, and for the ratios greater than r_c^{yx}, the curve possesses two maxima and one local minimum; note that at extremum values of HSIF, the SSIF is zero, as illustrated in Figs 4a and b. This phenomenon is depicted for three sets of (θ and α) values in Figs 5a,b,c, where the indicated values of r_c^{yx} are found numerically. Observe that, when θ and α are very small, r_c^{yx} is about 4, and for larger θ's and α's, r_c^{yx} takes on values other than 4.

For the case of small α and θ, for which (36) is valid, consider Fig. 5a where $\alpha = 0$ and $\theta = 0^\circ$. Then, for r^{yx} less than 4, the HSIF-curve has one maximum. As r^{yx} is increased, the curvature of the curve approaches zero. At the critical value of $r_c^{yx} = 4$, the HSIF-curve has an almost zero curvature. As a result, at $r_c^{yx} = 4$, for a wide range of angle ω, the HSIF-curve is essentially a horizontal line. Therefore, HSIF is not maximum at a well-defined point. Hence, while ω_c is then *undetermined*, it is not *infinite*. This flatness of the HSIF-curve in this case indicates that, for a wide range of angle ω, the HSIF (which is a measure of the *hoop* stress around the crack tip) is almost constant for $r_c^{yx} = 4$. The "change of the curvature" and "constant valuedness" of HSIF simply stem from the elasticity solution of the stress field around the crack tip, unrelated to the K-based fracture criterion which must be established by experimental observations, assisted by theoretical results. As another example, Fig. 5b depicts a similar case where $\alpha = 0.1$ and $\theta = 0^\circ$. Here for $r_c^{yx} \approx 7$, the HSIF-curve begins to display a local minimum. Figure 5c is yet another example, where for $\alpha = 0.3$ and $\theta = 5^\circ$, we have $r_c^{yx} \approx 12$. Note that, in this case, no horizontal region of the type in Fig. 5a exists; see Figs 5b and 5c.

Table 1 compares the critical kink angles, $\omega_c(K_m)$, obtained from four different formulae for $\alpha = 0.02$ and $\theta = 2^\circ$ at various values of C_{yy}/C_{xx} (first row of Table 1). By

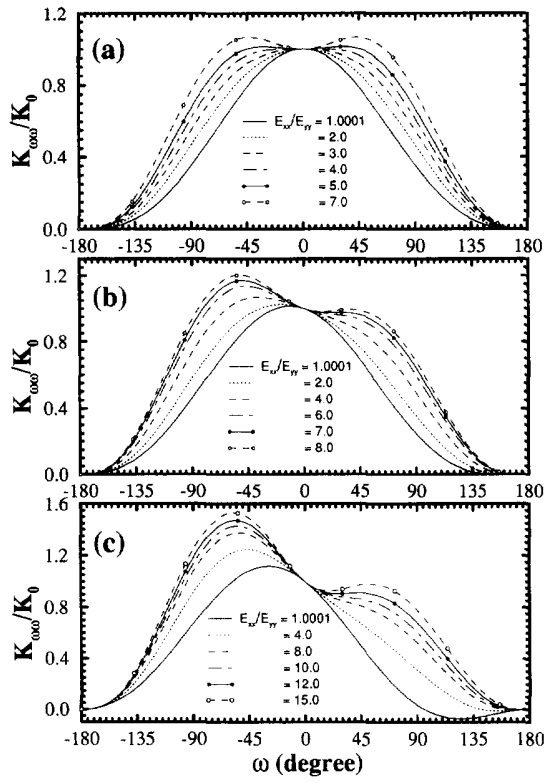

Fig. 5. Variation of HSIF vs ω for: (a) $\theta = 0°$, $\alpha = 0.0$ (pure tensile stress); (b) $\theta = 0°$, $\alpha = 0.1$; and (c) $\theta = 5°$, $\alpha = 0.3$.

maximizing (33) with respect to the kink angle, the angle at which $K_I^{(k)}$ (the stress intensity factor at the tip of a vanishingly small kink) is maximum is found (second row). Then (26) is used to obtain the kink angle which renders HSIF maximum (third row). As is seen, these two sets of critical kink angles (second and third rows) are very close. It seems that this is a result which holds for a rather broad range of parameters and loading conditions.

We also compare the values of $\omega_c(K_m)$ obtained from (26) of the present work (fourth row) with the values obtained from eqn (84) of Gao and Chiu (1992) (fifth row). Note that (84) is the linearized version of our (26) or (77) of Gao and Chiu (1992) when it is maximized with respect to the kink angle. For $\alpha = 0.02$ and $\theta = 2°$, eqn (84) of Gao and Chiu (1992) are applicable, since the ratio α and the angle θ are very small. Table 1 shows that for r^{yx} less than 4, the results of (84) of Gao and Chiu (1992) are accurate. For $r^{yx} = 4$, on the other hand, eqn (84) gives unacceptable results (an *infinite* angle for ω). For r^{yx} greater than 4, furthermore, (84) does not predict the correct $\omega_c(K_m)$, but instead, inaccurately estimates the value of ω at the local minimum; (note that, at the local minimum of K_I, K_{II} (HSIF, SSIF in the present work) is zero which is the original condition used to obtain (84)). However, this local minimum is not of practical importance. The above observations

Table 1. The critical angle (in degrees) obtained from different formulas for $\alpha = 0.02$ and $\theta = 2°$

C_{xy}/C_{xx}	1	2	3	4	5	6	7	8	9
$\omega_c(K_m)^{(1)}$	−2.3	−3.9	−8.1	−22.5	−34.3	−40.3	−44.1	−46.8	−48.9
$\omega_c(K_m)^{(2)}$	−2.3	−3.9	−8.0	−21.2	−32.3	−38.2	−42.0	−44.8	−46.9
$\omega_c(K_m)^{(3)}$	—	—	—	—	10.1	5.1	3.6	2.8	2.3
$\omega_c(K_m)^{(4)}$	−2.3	−3.9	−8.6	∞	9.7	5.1	3.6	2.8	2.3

(1)From (33), i.e., the angle at which $K_I^{(k)}$ is maximum.
(2)From (26) or (77) of Gao and Chiu (1992), i.e., the angle at which $K_{\omega\omega}$ is maximum.
(3)From (26) for points of local minimum (for $C_{xy}/C_{xx} < 4$, there is no local minimum).
(4)From (84) of Gao and Chiu (1992), i.e., the linearized version of (26).

indicate that eqn (84) (for r^{vx} greater than 4) does not give the branch angle which simultaneously satisfies the zero-K_{II} (zero-SSIF) and maximum-K_I (maximum-HSIF) conditions.

It is hoped that the above results and comments will serve to clarify the roots of the negative conclusions arrived at by Gao and Chiu (1992) regarding the validity of the K-based fracture criteria. Notwithstanding this, the relevance of the K-based and other considered competing fracture criteria must be established through controlled experiments.

CONCLUSIONS

In this study, crack kinking in an infinite, homogeneous, anisotropic, linearly elastic plane containing a central main crack has been investigated. At the tip of this main crack, two stress intensity factors are defined, one associated with the hoop stress, called the hoop stress intensity factor (HSIF), and the other associated with the shear stress, called the shear stress intensity factor (SSIF). The results and observations of this work are compared with those of Obata *et al.* (1989) for vanishingly small kinks, and then, with some of the results of Gao and Chiu (1992). The following conclusions are obtained:

(1) The HSIF and SSIF are more descriptive alternatives to the commonly used Modes I and II stress intensity factors defined at the tip of the main crack.

(2) In the problem of crack kinking in anisotropic solids, for small kink angles (between -8° and $+8^\circ$), these hoop and shear stress intensity factors yield Modes I and II stress intensity factors defined at the tip of a vanishingly small kink emanating from the tip of the main crack ($K_I^{(k)}$ and $K_{II}^{(k)}$) with less than 1% error. The range (-8° and $+8^\circ$) widens or narrows as anisotropy decreases or increases, respectively. The 1% error may increase to 5% for larger kink angles (up to about 30°). Therefore, for relatively small kink angles, the HSIF and SSIF are the physical quantities which correlate the fields just before crack kinking to those just after crack kinking. It is worthy to mention that, we have observed that the kink angles which render HSIF and $K_I^{(k)}$ maximum are close even when the magnitude of these two quantities are different by 100% or more.

(3) In contrast to (2), for the isotropic case, for all practical purposes, the prediction of the kink angle by the maximum-HSIF criterion favorably agrees with the prediction of the maximum-$K_I^{(k)}$ fracture criterion.

(4) In addition to (2), for small kink angles, all field quantities at the tip of a vanishingly small kink can be obtained from the hoop and shear stress intensity factors that exist at the tip of the initial main crack prior to kinking. This is valid for rather large kink angles when the material is isotropic.

(5) It is shown that Gao and Chiu's (1992) conclusions on inappropriateness of the K-based fracture criterion stem from their inappropriate linearization of highly nonlinear expressions. For example, the branch angle ω_c at a compliance ratio of "4" is *not* infinite, contrary to the conclusions of Gao and Chiu (1992), rather it is *undetermined.* Indeed, ω_c remains finite for any anisotropy and any loading conditions.

(6) The K-based fracture criterion may still be wanting in the sense that its validity has to be verified by experimental results. The maximum-HSIF and the zero-SSIF fracture criteria (K-based fracture criteria) are stress-based criteria, representing the stress field near the crack tip. Whether or not the "hoop and shear stress intensity factors" are appropriate parameters for crack propagation prediction has to be verified through coordinated experiments. Similarly, the G-based fracture criterion (which is energy-based) should be assessed through experimental results.

This study emphasizes the fact that, in the case of general anisotropy, prediction of the mode and direction of crack kinking requires consideration of material symmetry, as well as the asymmetry in the loading and geometry. Therefore, in the presence of any asymmetries, i.e., asymmetry in geometry, loading, and material orientation, the body response is generally asymmetric. In addition, the orientation dependence of the fracture

resistance in the material (fracture resistance is also an anisotropic quantity in most anisotropic solids, especially in single crystals) makes the study of crack kinking more complex.

Acknowledgements—This work has been supported in part by ARO under Grant No. DAAL03-92-K-0002, to the University of California, San Diego. Special thanks are due to Professor Makoto Obata for helpful comments.

REFERENCES

Azhdari, A. (1995). Fracturing in anisotropic brittle solids. Ph. D. dissertation, University of California, San Diego.

Chatterjee, S. N. (1975). The stress field in the neighborhood of a branched crack in an infinite elastic sheet. *Int. J. Solids Structures* **11,** 521–538.

Cotterell, B. and Rice, J. R. (1980). Slightly curved or kinked cracks. *Int. J. Fract.* **16,** 155–169.

Erdogan, F. and Sih, G. C. (1963). On the crack extension in plates under plane loading and transverse shear. *J. of Basic Engng* **85,** 519–527.

Gao, H. and Chiu, C. (1992). Slightly curved or kinked cracks in anisotropic elastic solids. *Int. J. Solids Structures* **29,** 947–972.

Gerasoulis, A. (1982). The use of piecewise quadratic polynomials for the solution of singular integral equations of Cauchy type. *Comput. Math. Applications* **8,** 15–22.

Hayashi, K. and Nemat-Nasser, S. (1981a). Energy release rate and crack kinking under combined loading. *ASME J. Appl. Mech.* **48,** 520–524.

Hayashi, K. and Nemat-Nasser, S. (1981b). Energy release rate and crack kinking. *Int. J. Solids Structures* **17,** 107–114.

Karihaloo, B. L., Keer, L. M., Nemat-Nasser, S. and Oranratnachai, A. (1981). Approximate description of crack kinking and curving. *J. Appl. Mech.* **48,** 515–519.

Kitagawa, H. and Yuuki, R. (1975). Stress intensity factors for branched cracks in an infinite body in the two dimensional stress state. *Trans. JSME* **41,** 1641–1649.

Lekhnitskii, S. G. (1963). *Theory of Elasticity of an Anisotropic Elastic Body* (translated by P. Fern). Holden-Day, San Francisco.

Lo, K. K. (1978). Analysis of branched cracks. *J. Appl. Mech.* **45,** 797–802.

Miller, G. R. and Stock, W. L. (1989). Analysis of branched interface cracks between dissimilar anisotropic media. *J. Appl. Mech.* **56,** 844–849.

Nemat-Nasser, S. (1980). On stability of the growth of interacting cracks, and crack kinking and curving in brittle solids. In *Numerical Methods in Fracture Mechanics* (eds D. R. J. Owen and A. R. Luxmoore). Pineridge Press, Swansea, United Kingdom, pp. 687–706.

Nemat-Nasser, S. and Horii, H. (1982). Compression induced non-planar crack extension with application to splitting, exfoliation and rockburst. *J. Geophysical Res.* **87,** 6805–6821.

Nemat-Nasser, S. and Hori, M. (1987). Toughening by partial or full bridging of cracks in ceramics and fiber reinforced composites. *Mech. Mater.* **6,** 245–269.

Obata, M., Nemat-Nasser, S. and Goto, Y. (1989). Branched cracks in anisotropic elastic solids. *J. Appl. Mech.* **56,** 858–864.

Otsuka, A., Mori, K., and Miyata, T. (1975). The condition of fatigue crack growth in mixed mode condition. *Engng Fract. Mech.* **7,** 429–439.

Savin, G. N., (1961). *Stress Concentrations around Holes*. Pergamon Press, Oxford.

Sih, G. C., Paris, P. C. and Irwin, G. R. (1965). On cracks in rectilinearly anisotropic bodies. *Int. J. Frac. Mech.* **1,** 189–203.

Sumi, Y., Nemat-Nasser, S. and Keer, L. M. (1983). On crack branching and curving in a finite body. *Int. J. Fract.* **21,** 67–79.

Williams, M. L. (1957). On the stress distribution at the base of a stationary crack. *ASME J. Appl. Mech.* **24,** 109–114.

Wu, C. H. (1979a). Fracture under combined loads by maximum-energy-release rate criterion. *J. Appl. Mech.* **46,** 553–558.

Wu, C. H. (1979b). Explicit asymptotic solution for the maximum energy-release-rate problem. *Int. J. Solids Structures* **15,** 561–566.